Electrochemistry

Deutsche Ausgabe: DOI: 10.1002/ange.201502396
Internationale Ausgabe: DOI: 10.1002/anie.201502396

High-Yield Electrosynthesis of Hydrogen Peroxide from Oxygen Reduction by Hierarchically Porous Carbon**

Yanming Liu, Xie Quan, Xinfei Fan, Hua Wang, and Shuo Chen*

Abstract: *H_2O_2 production by electroreduction of O_2 is an attractive alternative to the current anthraquinone process, which is highly desirable for chemical industries and environmental remediation. However, it remains a great challenge to develop cost-effective electrocatalysts for H_2O_2 synthesis. Here, hierarchically porous carbon (HPC) was proposed for the electrosynthesis of H_2O_2 from O_2 reduction. It exhibited high activity for O_2 reduction and good H_2O_2 selectivity (95.0–70.2 %, most of them >90.0 % at pH 1–4 and >80.0 % at pH 7). High-yield H_2O_2 generation has been achieved on HPC with H_2O_2 concentrations of 222.6–62.0 mmol L^{-1} (2.5 h) and corresponding H_2O_2 production rates of 395.7–110.2 mmol h^{-1} g^{-1} at pH 1–7 and −0.5 V. Moreover, HPC was energy-efficient for H_2O_2 production with current efficiency of 81.8–70.8 %. The exceptional performance of HPC for electrosynthesis of H_2O_2 could be attributed to its high content of sp^3-C and defects, large surface area and fast mass transfer.*

Hydrogen peroxide is a potential energy carrier and an environmentally friendly oxidant for various chemical industries and environmental remediation. It is manufactured industrially by the anthraquinone process, an indirect batch method requiring sequential hydrogenation, oxidation of anthraquinone molecules, and extraction of H_2O_2 from organic solvents. However, this multistep method is energy-intensive and difficult for in situ H_2O_2 production.[1] Considerable efforts have been dedicated to develop efficient and on-site H_2O_2 production methods, which can not only considerably reduce the cost for H_2O_2 synthesis, transport, storage, and handling but also facilitate the subsequent application process. Direct synthesis of H_2O_2 has been achieved from H_2 and O_2 under plasma[2] or on various catalysts.[3] These methods offer a continuous mode for H_2O_2 production and enable the decentralized production. However, they suffer from potential explosion of H_2/O_2 gas mixture. Another alternative method is the electroreduction of O_2 through a two-electron pathway, which enables the in situ production of H_2O_2 at moderate temperature and atmospheric pressure while avoiding the danger of explosion.[4] Moreover, if H_2O_2 production is performed in a fuel cell, it is possible to recover the energy released during reaction.[5] For H_2O_2 production from electroreduction of O_2, it requires an active and cost-effective electrocatalyst which selectively reduces O_2 to H_2O_2 (two-electron pathway) over H_2O (four-electron pathway). Many potential electrocatalysts have been exploited for H_2O_2 production, including noble metals, metal alloys, and carbon materials.[4,6] Oxygen reduction on metal alloys such as Pd–Au and Pt–Hg proceeds primarily through the two-electron pathways with selectivity of 70.8–92.5 % (0.1–0.3 V vs. RHE, pH 1).[4,6a] However, the limited supply of noble metals hinders their application. Carbon materials are a promising alternative for H_2O_2 electrosynthesis due to their high abundance, low cost, and electroreduction activity. It has been found that carbon fibers, graphite, and N-doped porous carbon are active for H_2O_2 production with production rates of 1.67–121.5 mmol h^{-1} g^{-1} and current efficiencies of 26.5–65.2 % (pH 1–7), and their performance is related to material structure and doping.[6b,c,7] Despite the progress, it is still desirable to develop a novel carbon material with high activity and selectivity for H_2O_2 production.

Among various carbon materials, porous carbon materials are attractive for electrocatalysis due to their high surface area and large pore volume as well as good electrical conductivity.[8] In particular, porous carbon derived from the carbonization of metal–organic frameworks (MOFs) possesses unique properties. It presents a hierarchically porous structure with abundant micro-, meso-, or even macropores.[9] Such structure endows this material with plentiful exposed catalytic sites and shortened diffusion paths,[10] which are beneficial for H_2O_2 production from O_2 reduction. When carbonization is performed under H_2 even at atmospheric pressure, introduction of defect sites and transferring sp^2-C to sp^3-C will be promoted by a H_2 atmosphere and capillary pressure resulting from the micro-, mesoporous structure.[11] Both defects and sp^3-C can act as active sites for reactant adsorption or reaction during the electrocatalytic process[12] and thereby may improve the kinetics of oxygen reduction. However, their correlation with H_2O_2 production has not been elucidated. Here, we reported an economical and efficient electrocatalyst, hierarchically porous carbon (HPC) derived from MOF carbonization under H_2, for the selective electrosynthesis of H_2O_2 from O_2 at pH 1–7. The effect of defects and sp^3-C on H_2O_2 production performance is discussed.

HPC was prepared by a two-step method: hydrothermal synthesis of MOF-5 (using zinc nitrate and terephthalic acid)

[*] Y. M. Liu, Prof. X. Quan, X. F. Fan, Dr. H. Wang, Dr. S. Chen
Key Laboratory of Industrial Ecology and Environmental Engineering (Ministry of Education, China), Faculty of Chemical Environmental and Biological Science and Technology
Dalian University of Technology
Dalian 116024 (China)
E-mail: quanxie@dlut.edu.cn

[**] This work was supported by the National Basic Research Program of China (2011CB936002), the National Natural Science Foundation of China (21437001), and PCSIRT 13R05.

Supporting information for this article is available on the WWW under http://dx.doi.org/10.1002/anie.201502396.

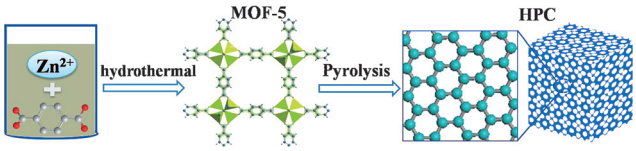

Figure 1. Schematic illustration of HPC preparation.

at 100 °C for 12 h, 24 h, or 36 h and subsequent carbonization of MOF-5 at 1100 °C for 5 h under H_2 atmosphere (Figure 1). The HPCs derived from MOF-5 with hydrothermal treatment times of 12 h, 24 h, and 36 h were named HPC-H12, HPC-H24, and HPC-H36, respectively. As a comparison, MOF-5 (24 h) was also annealed under Ar and the resulting product was named HPC-Ar24. SEM and TEM images (Figures 2 and

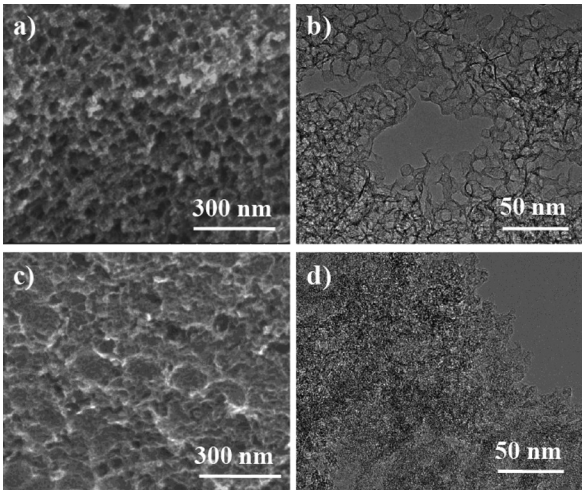

Figure 2. a) SEM and b) TEM images of HPC-H24; c) SEM and d) TEM images of HPC-Ar24.

S1) show the mesoporous structure of HPC-H12 and HPC-H36, whereas HPC-H24 possesses hierarchically porous features with interconnected mesopores and macropores. Compared with HPC-Ar24, HPC-H24 exhibits a much larger pore size and higher surface pore density, implying that carbonization under H_2 is correlated to its enlarged pore size and surface pore density relative to HPC-Ar24. These results show that the porous structure of HPC can be adjusted by changing the time for the hydrothermal treatment of the precursor and the carbonization conditions.

The surface area and porosity are two of the important factors generally related to the electrocatalytic performance of electrocatalysts, which has been examined by nitrogen adsorption–desorption isotherms (Figure 3a and Table S1). The BET surface areas of HPC-H12, HPC-H24, and HPC-H36 are 1635 $m^2 g^{-1}$, 2130 $m^2 g^{-1}$, and 1746 $m^2 g^{-1}$, respectively, demonstrating that HPC-H24 possesses the highest surface area among the three electrocatalysts. As expected, the BET surface area of HPC-H24 is also higher than that of HPC-Ar24 (1679 $m^2 g^{-1}$). Density functional theory (DFT) pore size distribution (Figure S2a) confirms the hierarchically porous structure of HPCs. The total pore volume of HPC-H24

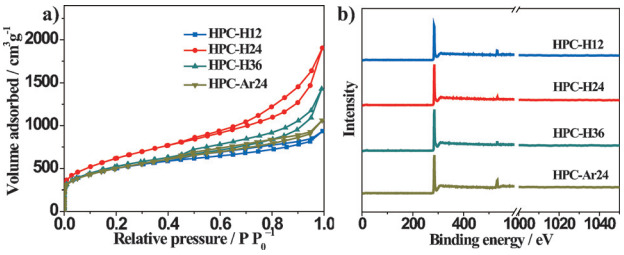

Figure 3. a) Nitrogen adsorption–desorption isotherms and b) XPS spectrum.

is 2.94 $cm^3 g^{-1}$, which is much larger than those of the others (1.45–2.21 $cm^3 g^{-1}$). In addition, the micropore volumes of these four HPCs are nearly the same (0.59–0.64 $cm^3 g^{-1}$, Figure S2b), indicating that carbonization under H_2 can significantly improve the pore volume of meso- and/or macropores. The X-ray diffraction (XRD) spectrum of HPCs (Figure S3) displays two weak peaks at about 25° and 44°, which are assigned to the (002) and (101) planes of carbon, respectively. No discernable peak related to a Zn impurity (1015–1050 eV) is observed from X-ray photoelectron spectroscopy (XPS, Figure 3b). The absence of Zn in HPCs was further confirmed by inductively coupled plasma atomic emission spectroscopy analysis, which was attributed to Zn evaporation during carbonization at a temperature higher than its boiling point (908 °C).[13] It demonstrates that carbonization yields a pure porous carbon.

The oxygen reduction activity of HPCs was first examined by cyclic voltammetry (CV) in Ar- or O_2-saturated solution. As shown in Figure 4a (pH 1) for all four HPC electro-

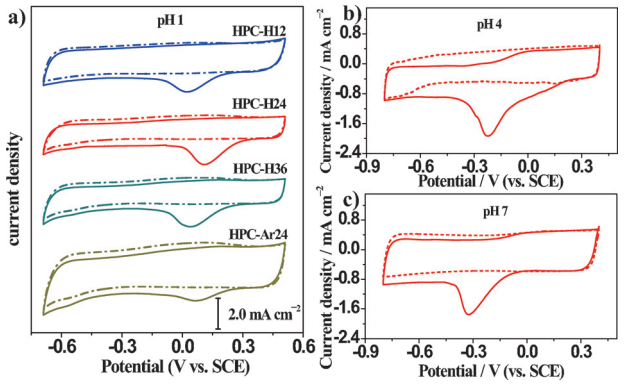

Figure 4. CV curves of HPCs in Ar- (dash line) or O_2-saturated (solid line) solution with a scan rate of 10 $mV s^{-1}$: a) HPC-H12, HPC-H24, HPC-H36, and HPC-Ar24 at pH 1; b) HPC-H24 at pH 4; c) HPC-H24 at pH 7.

catalysts, well-defined reduction peaks appear in the CV curves measured in O_2-saturated solution, whereas quasi-rectangular voltammograms without any noticeable peaks are obtained in Ar-saturated solution, indicating the pronounced electrocatalytic activity of HPCs for oxygen reduction. The peak potential of HPC-H24 for oxygen reduction is 0.12 V, which is more positive than those of HPC-H12 (0.03 V), HPC-H36 (0.06 V), and HPC-Ar24 (0.07 V). Meanwhile, HPC-H24

presents the highest peak current density. These results suggest that HPC-H24 is more active than HPC-H12, HPC-H36, and HPC-Ar24 for oxygen reduction. The performance of HPC-H24 is also better than those of HPC-H18 and HPC-H30 (Figure S4). To explore the electrocatalytic activity of HPC-H24 at higher pH values, its CV curves toward oxygen reduction were further measured at pH 4–7 (the pH-dependent reduction potential plot is presented in Figure S5). A well-defined oxygen reduction peak centered at −0.19 V is observed on HPC-H24 at pH 4 (Figure 4b). Interestingly, HPC-H24 also exhibits high activity in neutral solution (Figure 4c), in which H_2O_2 is expected to be the most flexible form for application. These results indicate that HPC-H24 is highly active for oxygen reduction at a wide range of pH values.

To gain further insight into the mechanism of the oxygen reduction reaction on HPC-H24, rotating disk measurements were recorded in O_2-saturated solution. According to the Koutecky–Levich plot (Figure S6), electron transfer numbers at pH 1 are calculated to be 2.10–2.38 for HPC-H24 at −0.1 to −0.5 V, implying that the oxygen reduction reaction on HPC-H24 is dominated by a two-electron process with H_2O_2 as the final product. Interestingly, at pH 4 and 7, the reaction also mainly occurs through the two-electron pathway on HPC-H24 (Figures S7 and S8). The H_2O_2 selectivity of HPC-H24 is 80.9–95.0% in acidic solution (pH 1 and 4) and 70.2–85.1% in neutral solution (Figure 5). These values are comparable or

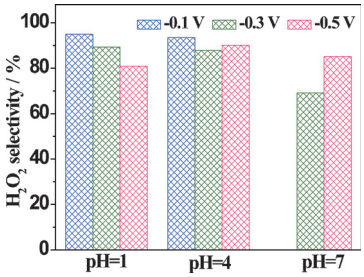

Figure 5. H_2O_2 selectivity of HPC-H24 at pH 1–7 and −0.1 to −0.5 V.

even better than those of electrocatalysts such as Pt–Hg/C,[4] Pd_xAu_{1-x}[6a], and Co–C[14] under similar conditions (Table S2), which are among the best reported recently. These results suggest that a high-yield electrosynthesis of H_2O_2 can be achieved on HPC-H24.

The excellent performance of HPC-H24 for H_2O_2 synthesis was verified by testing the real amount of H_2O_2 produced. Figure 6a–c shows the plots of accumulated H_2O_2 concentration versus electrolysis time, which reflects almost linear accumulation of H_2O_2 over electrolysis time at pH 1 and pH 4. When O_2 is electrochemically reduced on HPC-H24 at pH 1, the concentrations of H_2O_2 produced within 2.5 h are 95.8–222.6 mmol L^{-1} at −0.1 to −0.5 V. This translates to an H_2O_2 production rate of 1302.9–2249.4 mg L^{-1} h^{-1} at −0.1 to −0.3 V, which are 1–2 orders of magnitude higher than those of recently reported electrocatalysts[6b,15] under similar conditions (Table S3). Meanwhile, HPC-H24 gives a high mass yield for H_2O_2 production. The corresponding

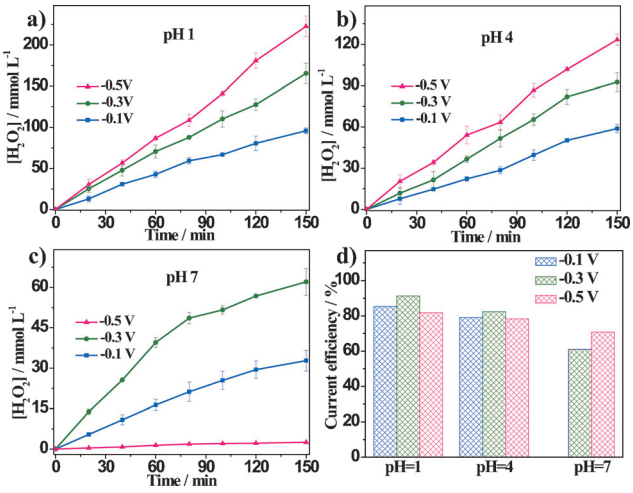

Figure 6. The concentration of H_2O_2 produced by HPC-H24 as a function of electrolysis time in solution with a) pH 1, b) pH 4, and c) pH 7; d) current efficiency of HPC-H24 for H_2O_2 production at −0.1 to −0.5 V and pH 1–7.

H_2O_2 production rate normalized by catalyst loading is 170.3–395.7 mmol h^{-1} g^{-1} on HPC-H24 at −0.1 to −0.5 V. It is worth noting that the H_2O_2 yield increases as the potential is negatively shifted at the potential range investigated. The same trend has been observed for H_2O_2 production at pH 4 and 7. As displayed in Figure 6b and c, H_2O_2 concentrations increase from 58.9 mmol L^{-1} (−0.1 V) to 123.4 mmol L^{-1} (−0.5 V, 219.3 mmol h^{-1} g^{-1}) at pH 4, and from 32.8 mmol L^{-1} (−0.3 V) to 62.0 mmol L^{-1} (−0.5 V, 110.2 mmol h^{-1} g^{-1}) at pH 7. Under the same potential, a lower pH value is beneficial for H_2O_2 production (consistent with the results reported[14,16]), which may be related to the participation of H^+ in H_2O_2 synthesis. Nevertheless, for H_2O_2 generation in neutral solution, HPC-H24 still outperforms non-noble-metal electrocatalysts reported recently[6c,14,15c] (Table S4). The good performance of HPC-H24 has been confirmed by using different electrolytes (Figure S9). Besides, HPC-H24 is stable during the successive electrosynthesis of H_2O_2 for six times (Figure S10). These results indicate the outstanding activity of HPC-H24 for H_2O_2 electrosynthesis in a wide range of pH values.

The current efficiency is one of the major concerns for electrocatalysis. Here, the current efficiency for H_2O_2 generation was also examined to further assess the performance of HPC-H24. As shown in Figure 6d, the current efficiency at pH 1 is 85.2–91.2% under a potential of −0.1 to −0.3 V. It increases initially as the potential is negatively shifted and slightly declines at −0.5 V (81.8%), which can be explained by the decreased H_2O_2 selectivity (Figure 5). As expected, HPC-H24 retains a high current efficiency (73.0–82.4%) for H_2O_2 production at pH 4. Although current efficiency at neutral solution is slightly declined (60.0–70.8%), HPC-H24 is still more energy-efficient than most electrocatalysts reported (26.5–52.5%).[6c,15c,16] These results indicate that a high energy efficiency can be achieved on HPC-H24 for H_2O_2 production at pH 1–7.

It is generally considered that an electrocatalyst with a high surface area is favorable for electrocatalytic reactions

because it can offer abundant catalytic sites. For HPCs carbonized under H_2, the BET surface areas follow the order of HPC-H24 > HPC-H36 > HPC-H12. The same trend has been observed for their electrocatalytic activity. Based on their similar oxygen reduction current density normalized by BET surface area, which are 0.124–0.130 $\mu A\,cm^{-2}$, it can be deduced that the oxygen reduction activity is mainly influenced by surface area for HPCs carbonized under H_2. However, HPC-Ar24 exhibits a much smaller normalized current density (0.100 $\mu A\,cm^{-2}$) compared with HPC-H24, suggesting that there are other factors contributed to the high activity of HPC-H24 except its high surface area.

To further understand the origin of its high activity, composition of HPC-H24 and HPC-Ar24 were analyzed by XPS and Raman spectroscopy. Both C 1s spectra of HPC-H24 and HPC-Ar24 can be deconvoluted to five peaks, which are associated with C=C (sp^2), C–C (sp^3), C–OH, C=O, and O=C–OH (Figure 7a and b). However, the peak area ratio of C–C/C=C for HPC-H24 (0.63) is significantly higher than that of HPC-Ar24 (0.25). It can be explained by the transformation of sp^2-C bonds to sp^3-C bonds after H_2 treatment at high temperature.[11,17] The Raman spectrum (Figure 7c) shows two peaks located at 1320 cm^{-1} (D band) and 1585 cm^{-1} (G band). The D band is associated with the introduction of sp^3-C bonds and structure defects on the edges or basal plane, whereas the G band is related to graphitic carbon. The intensity ratio of D band to G band (I_D/I_G) is 1.17 for HPC-H24, much higher than that for HPC-Ar24 (0.84). These results show that the content of sp^3-C bonds and defects is increased for HPC-H24 compared with HPC-Ar24. It has been reported that sp^3-C bonds and defects of carbon nanomaterials can act as active sites for the adsorption or reaction during the electrocatalytic process.[12b,18] These functions of sp^3-C bonds and defects may promote the oxygen reduction reaction and thereby facilitate H_2O_2 production. To evaluate these functions of sp^3-C bonds and defects, HPCs with I_D/I_G values of 0.84, 1.02, 1.17, and 1.31 were employed for H_2O_2 production. Figure 7d shows their H_2O_2 production rates normalized by BET surface area. When the I_D/I_G value of HPCs increases from 0.84 to 1.17, the H_2O_2 production rate is enhanced gradually, indicating a significant contribution of the sp^3-C bonds and defects for enhancing the electrocatalytic performance. However, the H_2O_2 production rate declines slightly by further increasing I_D/I_G to 1.31. According to the mechanism reported[4,19] and the electron transfer number measured, the H_2O_2 production on HPC-H24 occurred by an overall two-electron/two-proton reduction process (Eq. [S1–S4]: $O_2 \rightarrow {}^*HO_2 \rightarrow H_2O_2$). The defect sites are favorable for $^*HO_2$ accumulation[20] and this results in a high H_2O_2 selectivity, which may also contribute to the high performance of HPC-H24 for the electrosynthesis of H_2O_2 from O_2 reduction.

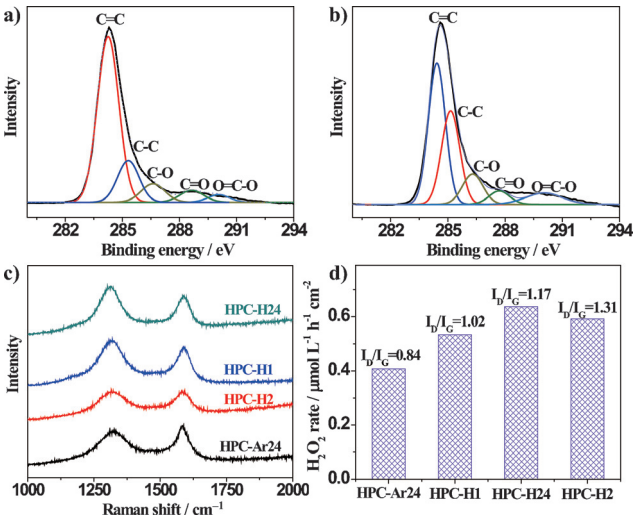

Figure 7. The C 1s XPS spectrum of a) HPC-Ar24 and b) HPC-H24; c) Raman spectra and d) H_2O_2 production rates (normalized by BET surface area, −0.3 V, pH 1) of HPC-Ar24, HPC-H24, HPC-H1, and HPC-H2.

Based on the aforementioned results, the following factors are responsible for the remarkable electrocatalytic performance of HPC-H24: 1) it has a high content of sp^3-C bonds and defects, which can act as reactive sites for oxygen adsorption or reduction during the electrocatalytic process; 2) its high surface area and 3D hierarchical porous structure provide plenty of exposed reactive sites, resulting in a large electroactive surface area for oxygen reduction; 3) its hierarchical pores can minimize the diffusion resistance for mass transport, favoring the efficient transfer of O_2, H^+/H_2O and the fast emission of H_2O_2; 4) benefiting from its defect sites, HPC-H24 has a high H_2O_2 selectivity.

In conclusion, a highly active and efficient electrocatalyst, HPC, has been presented for the electrosynthesis of H_2O_2 from O_2. It exhibited a good selectivity for the electrochemical reduction of O_2 to H_2O_2 in a wide range of pH values (1–7). Moreover, not only has a high-yield electrosynthesis of H_2O_2 been achieved on HPC with production rates of 395.7–110.2 $mmol\,h^{-1}\,g^{-1}$ (pH 1–7, −0.5 V), but also a high current efficiency of 70.8–81.8 % (pH 1–7, −0.5 V) was obtained from its H_2O_2 production tests. The outstanding performance of HPC resulted from its high content of sp^3-C bonds and defects, large surface area, and fast mass transport. All these features indicate that HPC is an attractive nonmetallic inorganic material for the electrosynthesis of H_2O_2. This work is also valuable for exploring related nonmetallic or all-carbon-based electrocatalysts for H_2O_2 production.

Keywords: electrocatalysis · electrochemistry · hydrogen peroxide synthesis · oxygen reduction · porous carbon

How to cite: *Angew. Chem. Int. Ed.* **2015**, *54*, 6837–6841
Angew. Chem. **2015**, *127*, 6941–6945

[1] J. M. Campos-Martin, G. Blanco-Brieva, J. L. Fierro, *Angew. Chem. Int. Ed.* **2006**, *45*, 6962–6984; *Angew. Chem.* **2006**, *118*, 7116–7139.
[2] Y. Yi, J. Zhou, H. Guo, J. Zhao, J. Su, L. Wang, X. Wang, W. Gong, *Angew. Chem. Int. Ed.* **2013**, *52*, 8446–8449; *Angew. Chem.* **2013**, *125*, 8604–8607.
[3] a) J. K. Edwards, J. Pritchard, L. Lu, M. Piccinini, G. Shaw, A. F. Carley, D. J. Morgan, C. J. Kiely, G. J. Hutchings, *Angew. Chem. Int. Ed.* **2014**, *53*, 2381–2384; *Angew. Chem.* **2014**, *126*, 2413–

2416; b) S. Shibata, T. Suenobu, S. Fukuzumi, *Angew. Chem. Int. Ed.* **2013**, *52*, 12327 – 12331; *Angew. Chem.* **2013**, *125*, 12553 – 12557; c) J. K. Edwards, B. Solsona, E. Ntainjua, A. F. Carley, A. A. Herzing, C. J. Kiely, G. J. Hutchings, *Science* **2009**, *323*, 1037 – 1041.
[4] S. Siahrostami, et al., *Nat. Mater.* **2013**, *12*, 1137 – 1143.
[5] I. Yamanaka, T. Onizawa, S. Takenaka, K. Otsuka, *Angew. Chem. Int. Ed.* **2003**, *42*, 3653 – 3655; *Angew. Chem.* **2003**, *115*, 3781 – 3783.
[6] a) J. S. Jirkovský, I. Panas, E. Ahlberg, M. Halasa, S. Romani, D. J. Schiffrin, *J. Am. Chem. Soc.* **2011**, *133*, 19432 – 19441; b) T. P. Fellinger, F. Hasche, P. Strasser, M. Antonietti, *J. Am. Chem. Soc.* **2012**, *134*, 4072 – 4075; c) I. Yamanaka, T. Murayama, *Angew. Chem. Int. Ed.* **2008**, *47*, 1900 – 1902; *Angew. Chem.* **2008**, *120*, 1926 – 1928.
[7] F. Yu, M. Zhou, L. Zhou, R. Peng, *Environ. Sci. Technol. Lett.* **2014**, *1*, 320 – 324.
[8] C. J. Shearer, A. Cherevan, D. Eder, *Adv. Mater.* **2014**, *26*, 2295 – 2318.
[9] J. K. Sun, Q. Xu, *Energy Environ. Sci.* **2014**, *7*, 2071 – 2100.
[10] D. W. Wang, D. Su, *Energy Environ. Sci.* **2014**, *7*, 576 – 591.
[11] C. H. Hsu, S. G. Cloutier, S. Palefsky, J. Xu, *Nano Lett.* **2010**, *10*, 3272 – 3276.
[12] a) A. Ueda, D. Kato, N. Sekioka, T. Kamata, R. Kurita, H. Uetsuka, Y. Hattori, S. Hirono, S. Umemura, O. Niwa, *Carbon* **2009**, *47*, 1943 – 1952; b) G. Zhong, H. Wang, H. Yu, F. Peng, *Electrochem. Commun.* **2014**, *40*, 5 – 8.
[13] G. Srinivas, V. Krungleviciute, Z. X. Guo, T. Yildirim, *Energy Environ. Sci.* **2014**, *7*, 335 – 342.
[14] A. Bonakdarpour, D. Esau, H. Cheng, A. Wang, E. Gyenge, D. P. Wilkinson, *Electrochim. Acta* **2011**, *56*, 9074 – 9081.
[15] a) R. B. Valim, R. M. Reis, P. S. Castro, A. S. Lima, R. S. Rocha, M. Bertotti, M. R. V. Lanza, *Carbon* **2013**, *61*, 236 – 244; b) A. Wang, A. Bonakdarpour, D. P. Wilkinson, E. Gyenge, *Electrochim. Acta* **2012**, *66*, 222 – 229; c) J. Choi, S. H. Hwang, J. Jang, J. Yoon, *Electrochem. Commun.* **2013**, *30*, 95 – 98.
[16] G. Zhang, S. Wang, S. Zhao, L. Fu, G. Chen, F. Yang, *Appl. Catal. B* **2011**, *106*, 370 – 378.
[17] L. T. Sun, J. L. Gong, D. Z. Zhu, Z. Y. Zhu, S. X. He, *Adv. Mater.* **2004**, *16*, 1849 – 1853.
[18] J. B. Jia, D. Kato, R. Kurita, Y. Sato, K. Maruyama, K. Suzuki, S. Hirono, T. Ando, O. Niwa, *Anal. Chem.* **2007**, *79*, 98 – 105.
[19] T. Murayama, I. Yamanaka, *J. Phys. Chem. C* **2011**, *115*, 5792 – 5799.
[20] J. C. Byers, A. G. Guell, P. R. Unwin, *J. Am. Chem. Soc.* **2014**, *136*, 11252 – 11255.

Received: March 14, 2015
Published online: April 20, 2015

